Earth and Planetary Science Letters 494 (2018) 164–171

Contents lists available at ScienceDirect

Earth and Planetary Science Letters

www.elsevier.com/locate/epsl

Experimental constraints on the sound velocities of cementite Fe_3C to core pressures

Bin Chen [a,*], Xiaojing Lai [a,b], Jie Li [c], Jiachao Liu [c], Jiyong Zhao [d], Wenli Bi [d], E. Ercan Alp [d], Michael Y. Hu [d], Yuming Xiao [e]

[a] Hawaii Institute of Geophysics and Planetology, University of Hawaii at Manoa, Honolulu, HI, USA
[b] Department of Geology and Geophysics, University of Hawaii at Manoa, Honolulu, HI, USA
[c] Department of Earth and Environmental Sciences, University of Michigan, Ann Arbor, MI, USA
[d] Advanced Photon Source, Argonne National Laboratory, Argonne, IL, USA
[e] HPCAT, Geophysical Laboratory, Carnegie Institution of Washington, Argonne, IL, USA

ARTICLE INFO

Article history:
Received 6 November 2017
Received in revised form 2 April 2018
Accepted 1 May 2018
Available online 17 May 2018
Editor: B. Buffett

Keywords:
iron carbide
inner core
magnetic transition
Poisson's ratio
compressional-wave velocity
shear-wave velocity

ABSTRACT

Sound velocities of cementite Fe_3C have been measured up to 1.5 Mbar and at 300 K in a diamond anvil cell using the nuclear resonant inelastic X-ray scattering (NRIXS) technique. From the partial phonon density of states (pDOS) and equation of state (EOS) of Fe_3C, we derived its elastic parameters including shear modulus, compressional (V_P) and shear-wave (V_S) velocities to core pressures. A pressure-induced spin-pairing transition in the powdered Fe_3C sample was found to occur gradually between 10 and 50 GPa by the X-ray Emission Spectroscopy (XES) measurements. Following the completion of the spin-pairing transition, the V_P and V_S of low-spin Fe_3C increased with pressure at a markedly lower rate than its high-spin counterpart. Our results suggest that the incorporation of carbon in solid iron to form iron carbide phases, Fe_3C and Fe_7C_3, could effectively lower the V_S but respectively raise the Poisson's ratio by 0.05 and 0.07 to approach the seismically observed values for the Earth's inner core. The comparison with the preliminary reference Earth model (PREM) implies that an inner core composition containing iron and its carbon-rich alloys can satisfactorily explain the observed seismic properties of the inner core.

1. Introduction

Iron (Fe) is widely accepted as the predominant constituent of the Earth's liquid outer core and solid inner core (Birch, 1964; Li and Fei, 2014). The core density deficit indicated the presence of considerable amount of lighter elements in the core, i.e., hydrogen (H), carbon (C), oxygen (O), silicon (Si), and sulfur (S) (Hirose et al., 2013; Li and Fei, 2014). Despite numerous concerted efforts from mineral physics, geochemistry, cosmochemistry, and seismology, the identity and abundance of the light constituents remain controversial. Alloying of one or more light elements with Fe at elevated pressure and temperature is found to substantially change the elastic properties such as density and sound velocities, essential to account for the core density deficit and sound velocity discrepancy (Hirose et al., 2013; Li and Fei, 2014). As such, understanding the high pressure–temperature (P–T) behaviors of liquid and solid Fe alloyed with lighter elements is integral to gaining insights into the compositions of Earth's various layers, the conditions under which the core and mantle segregated, the temperature regimes of the core and mantle, and the core–mantle interactions.

The plausibility of carbon as the principal light element in the Fe-dominant core originated partly from the observations of its high abundance as an element in the Solar System and carbonaceous chondrites and its high affinity to liquid Fe at the core–mantle segregation conditions (Wood, 1993; Wood et al., 2013; Chen and Li, 2016). As suggested by cosmochemical and geochemical studies, the evaporative loss of volatiles to space and the core formation may have caused the relative depletion of carbon in the bulk silicate Earth (BSE) in comparison with the Sun and carbonaceous chondrites (Wood et al., 2013; Chen and Li, 2016). The latter process involving the sequestration of Fe and lighter elements such as carbon from the mantle to the core was thought to have left behind isotopic signatures with elevated $^{56}Fe/^{54}Fe$ and $^{13}C/^{12}C$ ratio of the terrestrial basalts relative to chondrites and other terrestrial planetary bodies (Wood et al., 2013; Horita and Polyakov, 2015; Shahar et al., 2016).

The two common Fe carbide phases considered for the inner core are Fe_3C and Fe_7C_3 (Wood, 1993; Gao et al., 2008; Naka-

* Corresponding author.
E-mail address: binchen@hawaii.edu (B. Chen).

https://doi.org/10.1016/j.epsl.2018.05.002
0012-821X/

jima et al., 2009; Lord et al., 2009; Chen et al., 2014; Chen and Li, 2016). Cementite (Fe_3C) was initially proposed as the most likely carbide phase for the inner core, on the basis of thermodynamics calculations (Wood et al., 2013). At inner core boundary (ICB) condition, Fe_3C was considered to be the first phase to crystallize from an Fe–C–(S) liquid with merely 0.3% carbon (Wood et al., 2013). With a renewed interest more recently, the Fe–C–(S) system has been explored at higher pressures and temperatures (Nakajima et al., 2009; Dasgupta et al., 2009; Lord et al., 2009; Fei and Brosh, 2014). The revised phase diagrams of the Fe–C system from new high-pressure data suggested that Fe_7C_3 would be the first phase crystallizing from Fe–C liquids at ICB conditions (Lord et al., 2009; Nakajima et al., 2009; Fei and Brosh, 2014; Liu et al., 2016b), although experimental verifications at higher pressures are required. *Ab initio* calculations, however, reported conflicting results. Based on recent first-principles calculations on Fe_7C_3, the hexagonal Fe_7C_3 phase is suggested to become stable above 150 GPa, whereas the orthorhombic Fe_7C_3 phase is more stable below approximately 100 GPa (Raza et al., 2015). Zero kelvin theoretical structure prediction calculations have revealed that Fe_3C may adopt a new structure other than the cementite at core pressures and Fe_7C_3 may decompose to more stable stoichiometries such as Fe_2C and Fe_3C at inner core pressures (Bazhanova et al., 2012).

The magnetic transitions have been found to profoundly affect the physical properties of Fe alloys, such as density and sound velocities (Chen and Li, 2016). As a viable candidate that may exist in the inner core, Fe_3C has been reported to undergo magnetic transitions at high pressures. First-principles density functional theory (DFT) calculations have predicted that the ferromagnetic order in Fe_3C ceases at approximately 60 GPa (Vočadlo et al., 2002), but experiments suggest lower transition pressures (Lin et al., 2004b; Ono and Mibe, 2010). Recent DFT calculations suggested that a magnetic collapse of Fe_7C_3 occurring at approximately 67 GPa, though much lower values were reported by experimental studies (Chen et al., 2014; Liu et al., 2016a).

Mineral physics investigations of the candidate Fe carbides have indicated that the alloying of carbon with Fe may be necessary to explain the seismic observations of the core (Gao et al., 2009; Chen et al., 2012, 2014; Prescher et al., 2015; Chen and Li, 2016; Liu et al., 2016a). Recent studies suggested that the inner core may contain significant fraction of Fe_7C_3 in order to explain the anomalously low shear-wave (S-wave) velocity of the inner core (Chen et al., 2014) and its high Poison's ratio (v) (Prescher et al., 2015). There are still debates on which Fe carbide phase could be stable at the inner core conditions. Nevertheless, the sound velocity measurements of Fe carbides to core pressures are still limited. To date, the sound velocities measurements for Fe_3C have been limited to ~70 GPa (Gao et al., 2008; Fiquet et al., 2009). In this study, we determined both the V_P and V_S of Fe_3C up to 153 GPa at 300 K in a panoramic diamond anvil cell (DAC), employing the nuclear resonant inelastic X-ray scattering (NRIXS) technique. Our X-ray Emission Spectroscopy (XES) measurements revealed the pressure-induced magnetic or spin-pairing transition in Fe_3C, significantly influencing the elastic properties. We evaluated and discussed the effect of carbon on the acoustic properties of Fe under core conditions.

2. Experimental methods

2.1. Starting materials and high pressure experiments

The powered Fe_3C sample was synthesized from a mixture of 94.45% ^{57}Fe-enriched Fe powder (Cambridge Isotope Laboratories Inc., #FLM-1812-0) and graphite powder (Sigma-Aldrich, #282863) at an atomic ratio of Fe:C = 2.922:1 (Gao et al., 2009). The starting material was equilibrated at 2 GPa and 1373 K for 4 h in a multi-anvil press. The synthesized sample was probed by X-ray diffraction and conventional Mössbauer spectroscopy and found to be fine powder and pure Fe_3C (Gao et al., 2009).

The sample was then mechanically compressed to a pellet with a thickness of 15 μm. The sample assemblage was sandwiched by two NaCl layers and loaded into a sample chamber of ~75 μm in diameter drilled in cubic boron nitride (cBN) insert in an X-ray-transparent beryllium (Be) gasket. A panoramic DAC equipped with two 150 μm culet size double-bevel diamond anvils (8° angle) was used to generate high pressure, as described in Gao et al. (2009). The pressures of the sample at and below 107 GPa were determined by the ruby fluorescence of a few ruby spheres placed next to the sample (Mao et al., 1986) and the Raman spectra of the diamond anvil on top of the sample (Akahama and Kawamura, 2004). At pressures higher than 107 GPa, the pressures are solely determined by the Raman spectra of diamonds collected before and after each measurement. The discrepancies between ruby and diamond pressures are typically within ±5 GPa, even at 107 GPa in this study.

2.2. XES measurements at high pressures

The XES measurements of Fe_3C were performed in Sector 16-ID-D of the Advanced Photon Source (APS), Argonne National Laboratory. The technical details were described in Chen et al. (2014). The powdered sample was loaded in neon pressure medium and compressed in a panoramic DAC. Ruby spheres were loaded near the sample for pressure determination (Mao et al., 1986). The XES spectra for Fe_3C were normalized to unity in integrated intensity and analyzed using the Integrated Absolute Difference method (Vanko et al., 2006). The integrated spectra area differences between the K'_β satellite peaks of Fe_3C at high pressures and the low spin state reference spectrum of FeS_2 at 0 GPa. were calculated based on the integrated spectral area within 7035–7050 eV. The absolute values of the area differences were used as a proxy for the total spin momentum (Vanko et al., 2006; Chen et al., 2014).

2.3. NRIXS measurements at high pressures

The NRIXS experiments were performed at the Sector 3-ID-B of the APS, as described in Gao et al. (2009). The size of the X-ray beam was <10 μm in diameter, and the energy resolution was ~1 meV. At each pressure, NRIXS spectra were collected by tuning the X-ray energy within −70 to 95 meV around the ^{57}Fe nuclear transition energy of 14.4125 keV (corresponding to a wavelength of 0.86025 Å). Multiple NRIXS spectra were collected until sufficient counts were obtained at each pressure. NRIXS spectra were collected at 0, 26, 45, 65, 82, 107, 119, 130, and 153 GPa for one DAC loading. Typically, 6 to 26 NRIXS spectra were collected at each pressure from ambient to the highest pressure of 153 GPa in order to obtain sufficient counts for reliable velocity determination. The summed NRIXS spectrum at each pressure was then used to derive the phonon density of state (pDOS) (Sturhahn and Jackson, 2007).

The partial pDOS of Fe in Fe_3C was extracted from the NRIXS spectra at each pressure using the PHOENIX software program (Sturhahn, 2000). At a given pressure, Debye sound velocity (V_D) was derived from a parabolic fitting to the low-energy region of the pDOS using the following relationship:

$$\rho V_D = \frac{3\tilde{M}}{2\pi^2\hbar^3}\frac{E^2}{g(E)} \quad (1)$$

where ρ is the density of the ^{57}Fe-enriched sample, $g(E)$ is the pDOS as a function of energy E, $\hbar$ ($h/2\pi$) is the reduced Planck

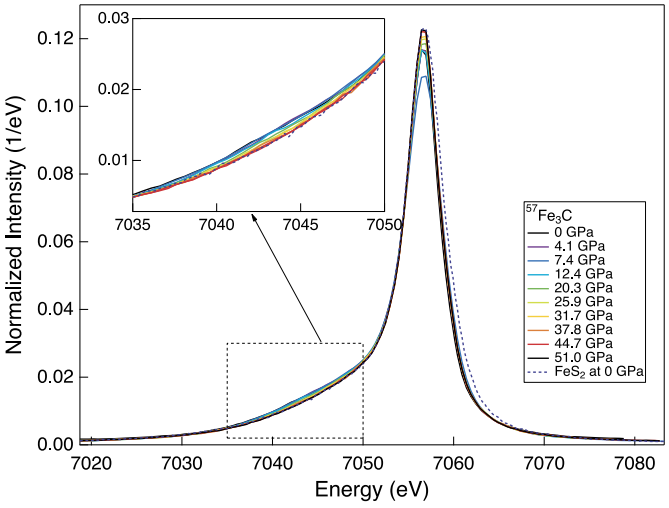

Fig. 1. Fe-K_β fluorescence spectra of Fe_3C up to 51 GPa and at 300 K from the XES measurements. The XES spectra were normalized to unity in integrated intensity. The top-left inset shows the satellite emission peak (K'_β) between 7035 and 7050 eV. The blue dashed line denotes the XES spectrum of the low-spin state reference FeS_2 at 0 GPa. (For interpretation of the colors in the figure(s), the reader is referred to the web version of this article.)

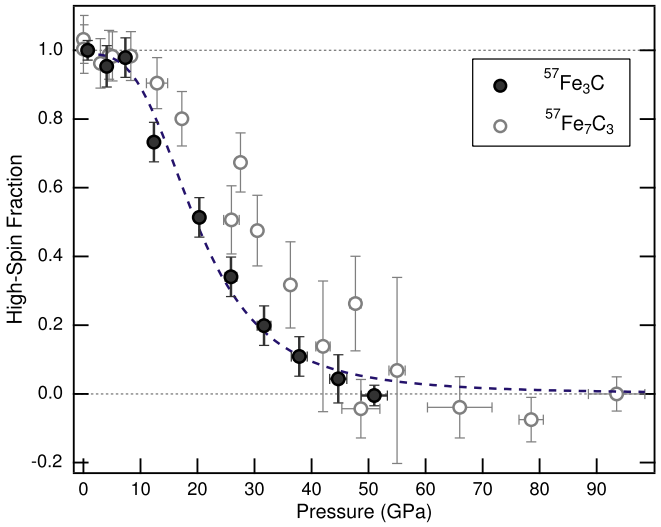

Fig. 2. High-spin fraction of Fe carbides as a function of pressure derived from the XES measurements. Solid black circles denote the high-spin fraction of Fe_3C (this study); open gray circles denote the high-spin fraction of Fe_7C_3 (Chen et al., 2014). See text for details.

constant and $\tilde{M}$ is the atomic mass of the resonant isotope (57 for ^{57}Fe) (Gao et al., 2009). Using the PHOENIX software, we derived V_D using the low energy range of the pDOS, where the parabolic relationship between $g(E)$ and E is valid (Fig. 4A) (Sturhahn, 2000; Sturhahn and Jackson, 2007) (see Fig. 4B for the determination of V_D at 119 GPa).

Densities and bulk moduli of Fe_3C were calculated from the EOS determined for the high-spin phase at lower than 50 GPa (Ono and Mibe, 2010) and the low-spin phase above 50 GPa (Sata et al., 2010), which were then used as the input parameters to calculate its V_P, V_S, and shear modulus G at a given pressure. The V_P and V_S of Fe_3C were calculated based on the following equations:

$$\begin{aligned} \frac{3}{V_D^3} &= \frac{1}{V_P^3} + \frac{2}{V_S^3}, \\ \frac{K_S}{\rho} &= V_P^2 - \frac{4}{3}V_S^2, \\ V_S^2 &= \frac{G}{\rho} \end{aligned} \tag{2}$$

3. Experimental results

3.1. Pressure-induced magnetic transitions of Fe_3C

Our XES measurements performed up to 51 GPa for Fe_3C show there exists notable K'_β satellite peak at pressures lower than ~50 GPa (Fig. 1). Similar to Fe_7C_3, the intensities of the K'_β peak remains almost constant up to ~10 GPa (Fig. 2), indicating a high-spin (HS) state with HS fraction of ~1.0 in Fe_3C. At >10 GPa, the integrated peak intensity continuously drops and disappears near ~50 GPa. This indicates that the total spin momentum of Fe approached zero at ~50 GPa and that Fe_3C underwent a gradual spin-pairing transition from HS to low-spin (LS) state across 10–50 GPa (Fig. 2).

Fe_3C may undergo tandem magnetic transitions at high pressures. Synchrotron Mössbauer spectroscopy (SMS) measurements by Gao et al. (2008) revealed a pressure-induced magnetic transition between 4.3 and 6.5 GPa. A magnetic transition at 9 GPa was suggested by X-ray magnetic circular dichroism (XMCD) measurements, which showed a continuous decrease of integrated intensity between ~6 and ~15 GPa (Acet et al., 2005). An earlier report on magnetic transition by XES measurements suggested a transition pressure of ~25 GPa (Lin et al., 2004b). However, the scatter of their data may be due to the limitations of the whole spectra analysis method as pointed out by Vanko et al. (2006). In the present study, our XES results showed a gradual spin-pairing transition at 10–50 GPa. It is plausible that the magnetic transition probed by SMS measurements by Gao et al. (2008) is a ferro- to parramagnetic transition. The XES results may reflect a gradual para- to non-magnetic transition or HS-to-LS transition at 10–50 GPa and Fe in Fe_3C may be totally in its LS state at >50 GPa.

3.2. Sound velocities of Fe_3C up to core pressures

The raw NRIXS data of Fe_3C up to core pressures are plotted in Fig. 3. Fig. 4 plotted the partial pDOS's derived from the NRIXS data at elevated pressures. The general feature of pDOS of Fe_3C is that the peaks shift to higher energy with increasing pressures. The room-temperature elastic properties of Fe_3C such as V_D, V_P, V_S, and G are experimentally determined up to 153 GPa (Fig. 5 and Table 1). At 0 GPa and 300 K, our determined V_D and V_S of the fine-powered Fe_3C are ~5% lower than those reported by Gao et al. (2008), whereas the V_D of the fine-powdered Fe_3C sample at ambient pressure by Gao et al. (2009) is almost identical to our value (Fig. 5). As pointed out by Gao et al. (2009), the discrepancy is likely due to the preferred orientation of the coarse polycrystalline grains of Fe_3C studied in Gao et al. (2008) and the large elastic anisotropy of Fe_3C (Mookherjee, 2011). Indeed, first principles calculations of single-crystal elasticity of Fe_3C revealed high elastic anisotropy with the fastest direction along the [110] direction for both V_P and V_S and the seismic anisotropies of the order of ~10% and ~25%, respectively (Mookherjee, 2011). The V_S as a function of pressure ($V_S(P)$) has similar shape than the V_D as a function of ($V_D(P)$), reflecting that NRIXS measurements are strongly sensitive to V_S and can thus place a tighter constraint on V_S relative to V_P (Sturhahn and Jackson, 2007).

From the sound velocity results, we found that the compressed Fe_3C demonstrates an unusual elastic behavior likely caused by the observed tandem magnetic transitions, similar to Fe_7C_3 (Chen et al., 2014). Our results revealed a pressure-induced elastic softening in compressed Fe_3C, manifested by a profound drop in V_S or V_D at ~50 GPa and likely due to the HS to LS transition. Looking at the $V_P(P)$ and $V_S(P)$ of Fe carbides and hcp-Fe, it is apparent that

Table 1
Elastic properties and Poisson's ratio (v) of Fe_3C at high pressures and at 300 K.

P[a] (GPa)	V_P (km s^{-1})	V_S (km s^{-1})	ρ[b] (g cm^{-3})	K_T[b] (GPa)	G (GPa)	v
0(0)[c]	5.67(.10)	2.84(.14)	7.809(.040)	167(2)	63(6)	0.29(.02)
26(1)	7.13(.07)	3.19(.08)	8.706(.009)	324(6)	89(4)	0.38(.01)
45(2)	7.83(.14)	3.31(.12)	9.160(.012)	427(8)	100(14)	0.39(.01)
65(3)	8.26(.04)	3.28(.04)	9.572(.010)	516(5)	103(3)	0.41(.01)
82(4)	8.55(.09)	3.38(.15)	9.876(.011)	572(6)	113(10)	0.41(.01)
107(5)	8.98(.05)	3.61(.05)	10.288(.013)	651(7)	134(4)	0.40(.01)
119(6)	9.15(.05)	3.67(.06)	10.474(.013)	689(7)	141(5)	0.40(.01)
130(7)	9.30(.09)	3.73(.15)	10.639(.014)	723(8)	148(12)	0.40(.01)
153(8)	9.59(.16)	3.84(.16)	10.967(.016)	793(9)	162(25)	0.41(.01)

[a] Pressures of the sample were calibrated by the ruby fluorescence of a few ruby spheres placed next to the sample (Mao et al., 1986) and the Raman spectra of the diamond anvil on top of the sample (Akahama and Kawamura, 2004) at and below 107 GPa and solely by Raman spectra of diamonds collected before and after each measurement at pressures higher than 107 GPa.

[b] Densities (ρ) and isothermal bulk moduli (K_T) of Fe_3C were calculated from the EOS's determined for high-spin phase at lower than 55 GPa by Ono and Mibe (2010) and low-spin phase above 55 GPa by Sata et al. (2010).

[c] Numbers in parentheses are uncertainties.

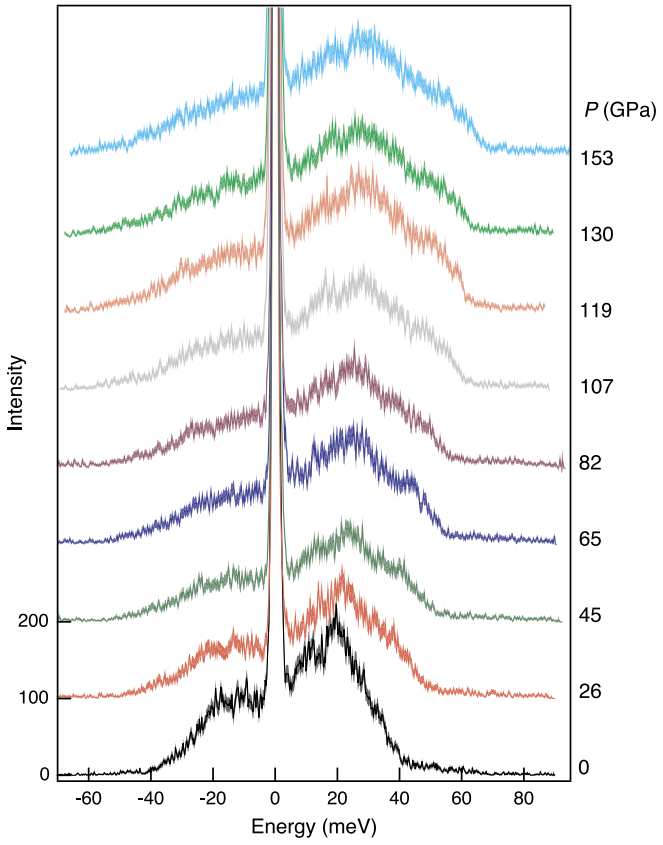

Fig. 3. NRIXS spectra of Fe in Fe_3C at high pressures and 300 K. The shaded margin of each spectrum represents statistical uncertainties. The spectra at high pressures are shifted vertically for clarity.

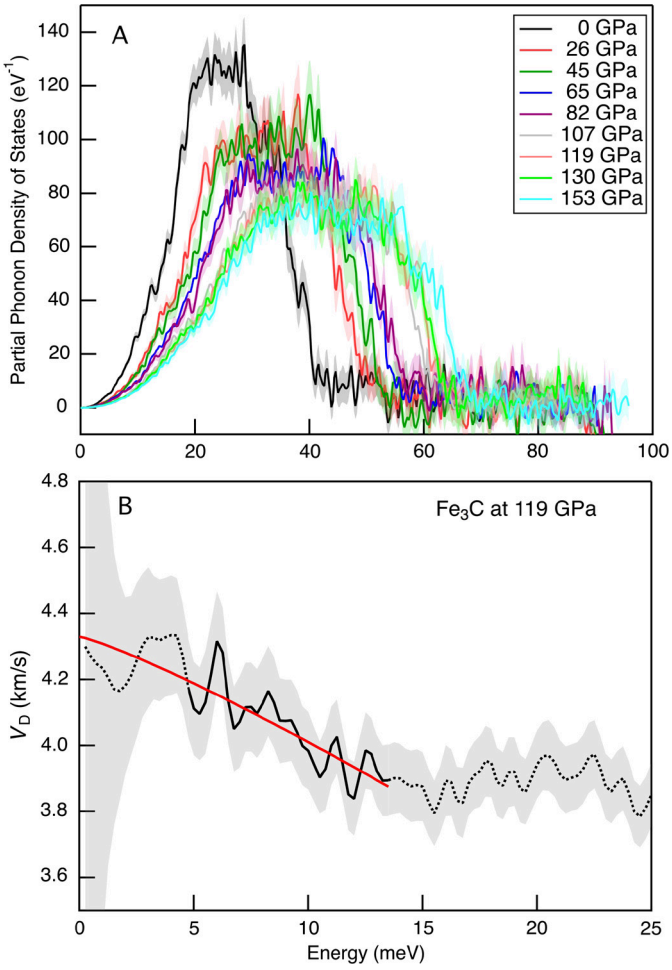

Fig. 4. (A) The derived partial phonon density of states (pDOS) of Fe in Fe_3C at pressures up to 153 GPa at 300 K. The shaded margin of each spectrum represents statistical uncertainties. (B) Representative determination of Debye sound velocity (V_D) of Fe_3C at 119 GPa. The low energy region (from 4.8 to 13.5 meV and denoted by black curve) of the pDOS was used to derive the V_D at $E = 0$. The gray shaded margin of the data represents statistical uncertainties. The data denoted by dotted curves were not used for the fit.

the alloying of carbon with Fe to form carbides can significantly depress both the V_S and V_P, especially after the spin transition (Fig. 5 and Fig. 6). The depression of velocities appear to be enhanced with increasing carbon content. Our results show that the alloying of carbon has much larger effect in reducing V_S than V_P.

Shear moduli (G) of Fe_3C demonstrated a linear relationship with pressure at >50 GPa, reaching approximately 160 GPa at the pressure of 168 GPa (Fig. 5B). Likewise, it was reported earlier by Chen et al. (2014) that the G of Fe_7C_3 only has a linear relationship with P at >50 GPa and reaches 125 GPa at the pressure of 160 GPa, lower than that of Fe_3C. At pressures higher than 55 GPa after the magnetic or spin transition, Fe_3C has larger K_T and is stiffer compared to Fe_7C_3 (Chen et al., 2014).

4. Discussion and geophysical implications

4.1. Effect of carbon alloying on sound velocities of Fe

In light of the tandem magnetic collapses of Fe_3C at 4.3–6.5 GPa and 10–50 GPa and their effect on the physical properties, we

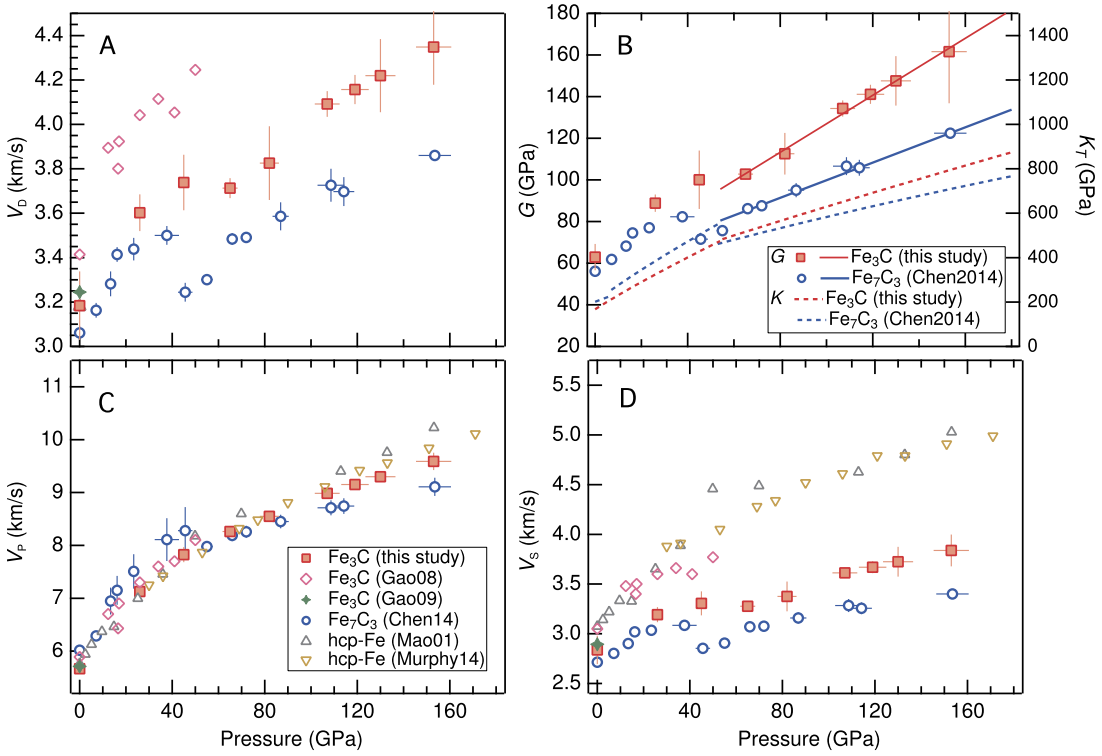

Fig. 5. Experimentally determined velocities and elastic moduli of Fe_3C up to 153 GPa and at 300 K, in comparison with Fe_7C_3 and Fe. (A) Debye sound velocity (V_D). (B) bulk moduli (K_T) and shear moduli (G), solid lines denote G and dashed lines denote K_T. K_T of Fe_3C were calculated based on the EOS by Ono and Mibe (2010) for the pressure range of 0–55 GPa and were calculated based on the EOS by Sata et al. (2010) for the pressures higher than 55 GPa. (C) Aggregate compressional-wave velocities V_P, (D) shear-wave velocities V_S of Fe_3C, in comparison with Fe_7C_3 (Chen et al., 2014) and Fe (Mao et al., 2001; Murphy et al., 2013). Red squares, results for Fe_3C (this study). Blue circles, results for Fe_7C_3 (Chen et al., 2014). Red dotted curve, isothermal bulk moduli (K_T) of Fe_3C: 0–55 GPa (Ono and Mibe, 2010), >55 GPa (Sata et al., 2010). Blue dotted curves, bulk moduli (K_T) of Fe_7C_3 (Chen et al., 2014). Solid curves, fits to the data for the non-magnetic phases of Fe_3C (red) and Fe_7C_3 (blue).

only use the experimental data for the LS-state Fe_3C at >50 GPa to extrapolate the seismic properties up to the inner core pressures, assuming the linear relationship between sound velocities and density (Birch, 1964). Under the inner core pressures, the extrapolated V_S of Fe_3C is ~39% above the PREM values of the inner core, whereas the extrapolated V_P of Fe_3C is ~6.7% higher than PREM values (Fig. 6).

Our results show that the alloying of carbon with Fe to form Fe carbides can significantly depress the sound velocities of Fe. The comparison of the results of Fe_3C with Fe_7C_3 indicated that increasing the carbon content lowers both the V_P and V_S of Fe profoundly. This is in contrast with the incorporation of Si in Fe; in that, the sound velocities increase with increasing Si content at high pressures (Lin et al., 2003a). The experimentally-determined and extrapolated sound velocities (V_P and V_S) of non-magnetic Fe_3C are noticeably higher than those of Fe_7C_3 under core conditions at room temperature (see Fig. 6). Compared to hcp-Fe (Mao et al., 2001; Murphy et al., 2013), the high-pressure non-magnetic phases of both Fe_3C and Fe_7C_3, relevant to the discussion of the inner core, evidently have much lower V_P and V_S.

The incorporation of carbon to hcp-Fe to form Fe carbides is a viable mechanism to lower the sound velocities of hcp-Fe, approaching the PREM values. Among all the investigated Fe alloys considered for the inner core, carbon is among the most effective elements in lowering the V_S to the seismic values (Chen et al., 2014; Chen and Li, 2016). Bearing in mind that all the measurements were performed at 300 K, the V_S results reported in this study represent a higher bound. The velocities of Fe alloys are expected to be depressed further with higher temperatures (Chen et al., 2014), so that a match with the PREM values could be realized by Fe carbides solely or a composite of Fe carbides and Fe.

It is crucial to know the effect of temperature on the sound velocities for the discussion of core composition. The estimates of the temperature dependence of V_S, however, remain largely elusive. Even for Fe or Fe–Ni alloys, the estimates range from an upper bound $-dV_S/dT = 3.7 \times 10^{-4}$ km s^{-1} K^{-1} for hcp-Fe at core pressures (Mao et al., 2001) to almost negligible high-temperature effect for *fcc* Fe–Ni alloy within the present experimental accuracy (Kantor et al., 2007). The aforementioned temperature effects on V_S are at most guesstimates. Additionally, experiments results showed that hcp-Fe did not follow Birch's law at high temperatures, and that sound velocities significantly decrease with temperature for a given density (Lin et al., 2005). Theoretical calculations also suggested that strong nonlinear high-temperature effect on the V_S of hcp-Fe under core conditions when the temperature is near the melting temperature of hcp-Fe (Martorell et al., 2013). For Fe_3C, Gao et al. (2011) suggested its V_S decreases with increasing temperature in a nonlinear fashion through high-temperature NRIXS measurements and the estimated average $-dV_S/dT$ of Fe_3C was approximately 1.5–1.7 $\times 10^{-4}$ km s^{-1} K^{-1} from 300 K to 1450 K at 46–47 GPa ($\rho = 8.8$ g cm^{-3}). The high-temperature effect was thought to be gradually suppressed by increasing density or pressure, likely due to the smaller thermal expansivity at higher densities and thus less anharmonic effect (Lin et al., 2005; Mao et al., 2012). Due to the sparse experimental data, the seemingly opposing effects of temperatures and pressures on dV_S/dT, and the possible premelting shear weakening of iron-rich alloys, we utilize a wide range of probable $-dV_S/dT$ from 1.0 to 3.7 $\times 10^{-4}$ km s^{-1} K^{-1} based on previous estimates (Mao et al., 2001; Kantor et al., 2007; Lin et al., 2005; Gao et al., 2011).

When the higher bound value of $-dV_S/dT = 3.7 \times 10^{-4}$ km s^{-1} K^{-1} is used, the calculated high-temperature V_S of Fe can account for the PREM values only in the case that the ICB tem-

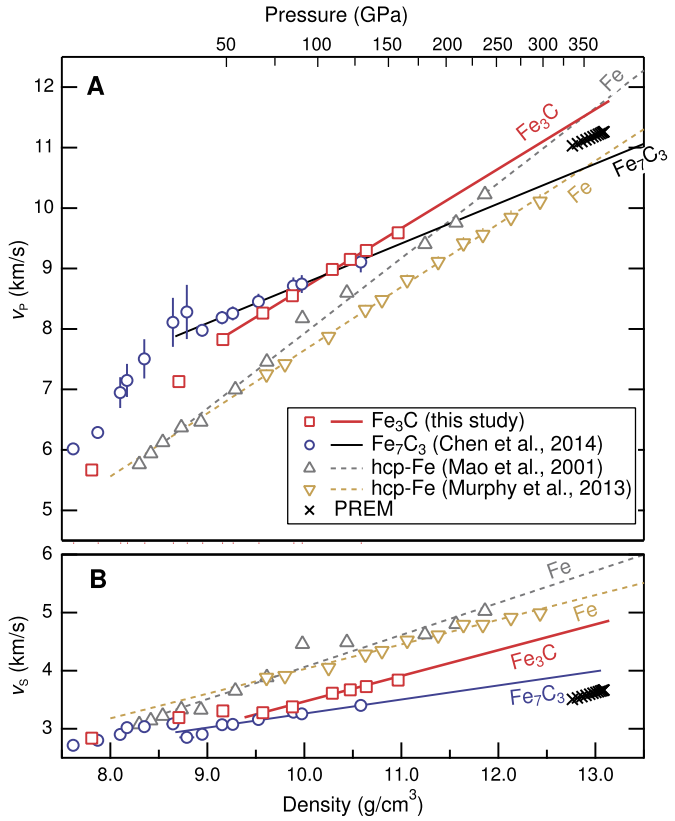

Fig. 6. Sound velocities of Fe carbides and Fe as a function of density. (A) Compressional and (B) shear wave velocities of Fe_3C (this study), Fe_7C_3 (Chen et al., 2014), Fe (Mao et al., 2001; Murphy et al., 2013). The pressure scale on the top axis is only for Fe_3C according to the EOS by Sata et al. (2010).

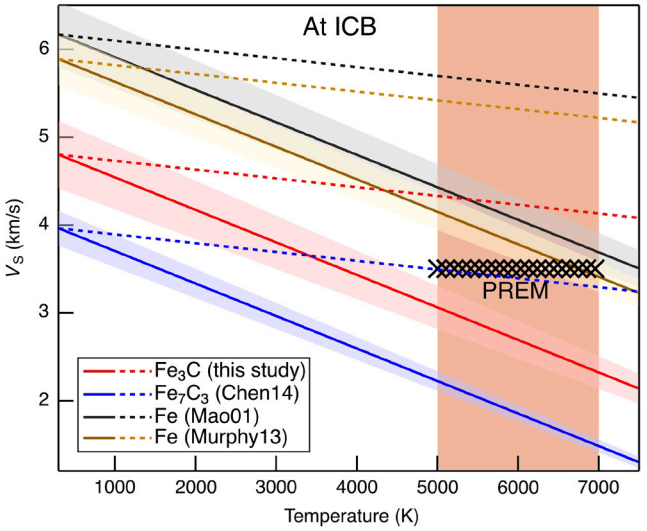

Fig. 7. V_S of Fe carbides and Fe at the inner core boundary conditions in comparison with PREM. Solid lines: The V_S at high temperatures for Fe_3C (this study), Fe_7C_3 (Chen et al., 2014), and Fe (Mao et al., 2001; Murphy et al., 2013) were estimated using an presumed upper bound for $-dV_S/dT = 3.7 \times 10^{-4}$ km s^{-1} K^{-1} (Mao et al., 2001). The dashed lines demonstrate the high-temperature V_S estimated using the lower bound $-dV_S/dT = 1.0 \times 10^{-4}$ km s^{-1} K^{-1} (Kantor et al., 2007). Shaded margins denote uncertainties. ICB-Inner Core Boundary.

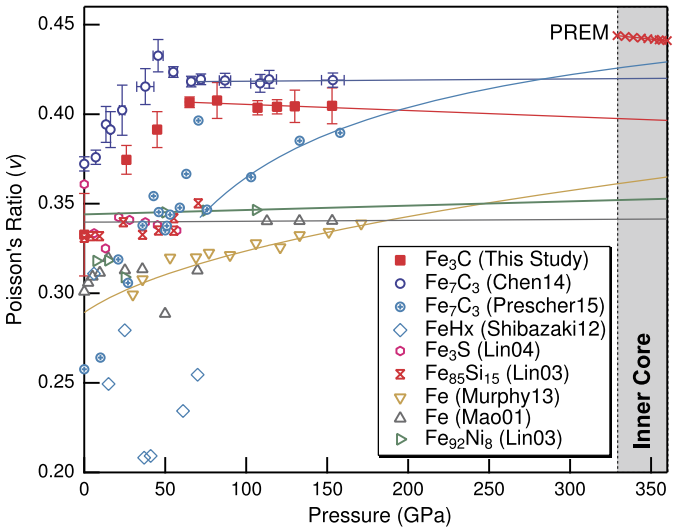

Fig. 8. Poisson's ratios of Fe alloys extrapolated up to the pressures of the Earth's inner core. Compared to other light elements, carbon significantly increases the Poisson's ratio significantly.

perature is close to 7000 K (Fig. 7). Given an ICB temperature of 5000 K, 3.0–4.5 wt% carbon are needed (Fig. 7). Given an ICB temperature of 6000 K, the carbon content becomes 1.2–2.6 wt.%. When the supposedly lower bound of $-dV_S/dT = 1.0 \times 10^{-4}$ km s^{-1} K^{-1} is used and the ICB temperature is at 5000–6000 K, we found that the inner core should be predominantly Fe_7C_3 with as high as 8.4 wt.% carbon and Fe_3C could not account for the low V_S of the inner core. Despite the ambiguity from the presumed high-temperature dependence, the anomalously low V_S values of the inner core almost warrant the presence of a constituting component with much lower V_S than Fe, i.e., Fe_3C or Fe_7C_3. It is very likely that the inner core contains considerable amount of carbon (>1 wt.%) to account for its anomalously low S-wave velocity. However, the estimates above would need to be revised if future experiments or calculations otherwise suggest the $-dV_S/dT$ of the iron carbides falls out of the presumed bounds.

4.2. Poisson's ratios of Fe alloys and the inner core

One of the intriguing seismic properties of Earth's inner core is its extraordinary high Poisson's ratio (ν), on the order of ~0.44 at the ICB (Dziewonski and Anderson, 1981). The main mechanisms that have been proposed for the high ν of the inner core includes partial melting (Vočadlo, 2007), the premelting effect (Martorell et al., 2013), and the presence or dominance of Fe carbides in the inner core (Chen et al., 2014; Prescher et al., 2015). The melting of the top of the Earth inner core does not readily explain the high Poisson's ratio throughout the entire inner core. The preempting mechanism also requires $T \sim 0.99 T_m$ (where T_m is the melting temperature) throughout the entire inner core.

The ν of Fe and its alloys with nickel and light elements can be calculated from the ratio V_P/V_S by the following relationship:

$$\nu = \frac{3K_S - 2G}{2(3K_S + G)} = \frac{(V_P/V_S)^2 - 2}{2[(V_P/V_S)^2 - 1]}, \quad (3)$$

where their V_P and V_S up to the inner core pressures can be estimated by extrapolating from available mineral physics data using the empirical Birch's linear relationship between V_P and ρ (Birch, 1964). Although the empirical linear relationship was intended to apply only to V_P and ρ, we found $V_S(P)$ may also follow the Birch's linear relationship at room temperature according to the existing V_S data (i.e., Chen et al., 2014).

Fig. 8 plotted the Poisson's ratio of Fe_3C, along with various other Fe alloys. It is apparent that Fe carbides have the highest ratio amounting to the PREM values than any other Fe-light-element compounds. It is noted that for both Fe_7C_3 (Chen et al., 2014) and Fe_3C (this study) the Poisson's ratios possess little pressure dependence at pressures higher than 50 GPa, even showing a similar

negative pressure dependence comparable to that of PREM at inner core pressures.

The v values of other Fe alloys at high pressures mostly fall below 0.35 and Fe carbides are the exceptions (Fig. 8). The v values of Fe (Mao et al., 2001; Murphy et al., 2013) and Fe–Ni alloy (Lin et al., 2003b) at core pressures mostly fall below ~0.35. Experimental data of other Fe alloys such as Fe_3S (Lin et al., 2004a), $Fe_{85}Si_{15}$ (Lin et al., 2003b), and FeH_x (Shibazaki et al., 2012) are only available up to ~70 GPa, but indicative of v values lower than 0.35 at core pressures. Similar to Fe_7C_3, the v values for Fe_3C increase markedly with pressure up to 50 GPa and become flat likely due to the spin transition at approximately 50 GPa. The extrapolation of v to the inner core pressure gives values of 0.42 for Fe_7C_3 and 0.40 for Fe_3C. Seismic studies reported that the v of the inner core has a negative pressure dependence under the inner core pressures (Dziewonski and Anderson, 1981). This negative pressure dependence is indicated for Fe_7C_3 (Chen et al., 2014) and Fe_3C in this study. The v values by Prescher et al. (2015), however, show strong positive pressure dependence, opposite to the pressure dependence of v of the inner core from seismic observations (Fig. 8). A main source for the discrepancy could be different EOS for Fe_7C_3 and/or the different approaches to derive the sound velocities from the pDOS.

4.3. Geophysical implications

For the consideration of the Earth's core, we generally consider compositions only in the Fe-rich region of the Fe–C system, as the maximum carbon content in the core is estimated to be 6–7 wt.% (Dasgupta and Walker, 2008). For the Fe–C core composition model, the mineralogy of the inner core is controlled by the bulk carbon content of the core and the eutectic composition of the Fe–C system at the ICB pressure. When the Earth's liquid outer core cools down, the carbon-rich liquid core may crystallize Fe carbide(s) if the bulk carbon content is higher than 2.2 wt.%; less bulk carbon content may lead to the crystallization of Fe with dissolved carbon (Fei and Brosh, 2014). There is currently no consensus concerning the stable Fe carbide phase at the liquidus of the Fe–C system under the ICB conditions. Fe carbides of different stoichiometries and structures, Fe_3C, Fe_7C_3, and Fe_2C, have all been proposed as the stable phase at core conditions, according to the thermodynamic modelings and *ab initio* calculations (Lord et al., 2009; Nakajima et al., 2009; Fei and Brosh, 2014; Bazhanova et al., 2012; Raza et al., 2015).

The mechanisms proposed to explain the large discrepancy in V_S between Fe and the inner core include the presence of partial melt (Singh et al., 2000), texture effect (Antonangeli et al., 2004), premelting effect (Martorell et al., 2013), and the presence of light elements such as carbon (Chen et al., 2014; Prescher et al., 2015). The presence of carbon possesses great potential in accounting for the vast velocity discrepancy for the inner core by effectively reducing the V_S and increasing the Poisson's ratio. Further, the compositional model for the inner core should be capable of explaining the seismic anisotropy of the inner core (Song and Helmberger, 1993). Future experimental priorities need to include the identification of the stable Fe carbide phase at ICB conditions and measurements of the elastic anisotropy of Fe carbides.

Acknowledgements

The authors thank Jin Liu, Zeyu Li and Sergey Tkachev for their assistance with the synchrotron experiments. Sector 3 operations are supported in part by COMPRES, the Consortium for Materials Properties Research in Earth Sciences under National Science Foundation (NSF) Cooperative Agreement EAR-1606856. Use of the COMPRES-GSECARS gas loading system was supported by COMPRES under NSF Cooperative Agreement EAR-1606856 and by GSECARS through NSF grant EAR-1634415 and DOE grant DE-FG02-94ER14466. Portions of this work were performed at HP-CAT (Sector 16), Advanced Photon Source (APS), Argonne National Laboratory. HPCAT operations are supported by DOE-NNSA under Award No. DE-NA0001974, with partial instrumentation funding by NSF. This research used resources of the Advanced Photon Source, a U.S. Department of Energy (DOE) Office of Science User Facility operated for the DOE Office of Science by Argonne National Laboratory under Contract No. DE-AC02–06CH11357. B.C. acknowledges the support from NSF grants EAR-1555388 and EAR-1565708. J.L. acknowledges the support from NSF grants AST-1344133, EAR-1763189, Sloan Foundation Deep Carbon Observatory grant G-2017-9954. Y.X. acknowledges the support of DOE-BES/DMSE under Award DE-FG02-99ER45775. The paper benefited from helpful comments and suggestions by two anonymous reviewers.

References

Acet, M., Wassermann, E., Mathon, O., 2005. Magnetic instabilities in Fe_3C cementite particles observed with Fe K-edge X-ray circular dichroism under pressure. Phys. Rev. Lett. 94, 1576.

Akahama, Y., Kawamura, H., 2004. High-pressure Raman spectroscopy of diamond anvils to 250 GPa: method for pressure determination in the multimegabar pressure range. J. Appl. Phys. 96, 3748–3751.

Antonangeli, D., Occelli, F., Requardt, H., Badro, J., Fiquet, G., Krisch, M., 2004. Elastic anisotropy in textured hcp-iron to 112 GPa from sound wave propagation measurements. Earth Planet. Sci. Lett. 225, 243–251.

Bazhanova, Z.G., Oganov, A.R., Gianola, O., 2012. Fe–C and Fe–H systems at pressures of the Earth's inner core. Phys. Usp. 55, 489–497.

Birch, F., 1964. Density and composition of mantle and core. J. Geophys. Res. 69, 4377–4388.

Chen, B., Gao, L., Lavina, B., Dera, P., Alp, E.E., Zhao, J., Li, J., 2012. Magneto-elastic coupling in compressed Fe_7C_3 supports carbon in Earth's inner core. Geophys. Res. Lett. 39, L18301.

Chen, B., Li, J., 2016. Carbon in the core. In: Deep Earth. John Wiley & Sons, Inc., Hoboken, NJ, pp. 277–288.

Chen, B., Li, Z., Zhang, D., Liu, J., Hu, M.Y., Zhao, J., Bi, W., Alp, E.E., Ercan Alp, E., Xiao, Y., Chow, P., Li, J., 2014. Hidden carbon in Earth's inner core revealed by shear softening in dense Fe_7C_3. Proc. Natl. Acad. Sci. USA 111, 17755–17758.

Dasgupta, R., Buono, A., Whelan, G., Walker, D., 2009. High-pressure melting relations in Fe–C–S systems: implications for formation, evolution, and structure of metallic cores in planetary bodies. Geochim. Cosmochim. Acta 73, 6678–6691.

Dasgupta, R., Walker, D., 2008. Carbon solubility in core melts in a shallow magma ocean environment and distribution of carbon between the Earth's core and the mantle. Geochim. Cosmochim. Acta 72, 4627–4641.

Dziewonski, A.M., Anderson, D.L., 1981. Preliminary reference Earth model. Phys. Earth Planet. Inter. 25, 297–356.

Fei, Y., Brosh, E., 2014. Experimental study and thermodynamic calculations of phase relations in the Fe–C system at high pressure. Earth Planet. Sci. Lett. 408, 155–162.

Fiquet, G., Badro, J., Gregoryanz, E., Fei, Y., Occelli, F., 2009. Sound velocity in iron carbide (Fe_3C) at high pressure: implications for the carbon content of the Earth's inner core. Phys. Earth Planet. Inter. 172, 125–129.

Gao, L., Chen, B., Lerche, M., Alp, E.E., Sturhahn, W., Zhao, J., Yava, H., Li, J., 2009. Sound velocities of compressed Fe_3C from simultaneous synchrotron X-ray diffraction and nuclear resonant scattering measurements. J. Synchrotron Radiat. 16, 714–722.

Gao, L., Chen, B., Wang, J., Alp, E.E., Zhao, J., Lerche, M., Sturhahn, W., Scott, H.P., Huang, F., Ding, Y., Sinogeikin, S.V., Lundstrom, C.C., Bass, J.D., Li, J., 2008. Pressure-induced magnetic transition and sound velocities of Fe_3C: implications for carbon in the Earth's inner core. Geophys. Res. Lett. 35, L17306.

Gao, L., Chen, B., Zhao, J., Alp, E.E., Sturhahn, W., Li, J., 2011. Effect of temperature on sound velocities of compressed Fe_3C, a candidate component of the Earth's inner core. Earth Planet. Sci. Lett. 309, 213–220.

Hirose, K., Labrosse, S., Hernlund, J., 2013. Composition and state of the core. Annu. Rev. Earth Planet. Sci. 41, 657–691.

Horita, J., Polyakov, V.B., 2015. Carbon-bearing iron phases and the carbon isotope composition of the deep Earth. Proc. Natl. Acad. Sci. USA 112, 31–36.

Kantor, A.P., Kantor, I.Y., Kurnosov, A.V., Kuznetsov, A.Y., Dubrovinskaia, N.A., Krisch, M., Bossak, A.A., Dmitriev, V.P., Urusov, V.S., Dubrovinsky, L.S., 2007. Sound wave velocities of fcc Fe–Ni alloy at high pressure and temperature by mean of inelastic X-ray scattering. Phys. Earth Planet. Inter. 164, 83–89.

Li, J., Fei, Y., 2014. Experimental constraints on core composition. In: Holland, H.D., Turekian, K.K. (Eds.), Treatise on Geochemistry, second edition. Elsevier, Oxford, pp. 527–557.

Lin, J.-F., Sturhahn, W., Zhao, J., Shen, G., Mao, H.-K., Hemley, R.J., 2005. Sound velocities of hot dense iron: Birch's law revisited. Science 308 (5730), 1892–1894. https://doi.org/10.1126/science.1111724.

Lin, J.F., Campbell, A.J., Heinz, D.L., Shen, G., 2003a. Static compression of iron–silicon alloys: implications for silicon in the Earth's core. J. Geophys. Res. 108, 2045.

Lin, J.F., Fei, Y., Sturhahn, W., Zhao, J., Mao, H.k., Hemley, R.J., 2004a. Magnetic transition and sound velocities of Fe_3S at high pressure: implications for Earth and planetary cores. Earth Planet. Sci. Lett. 226, 33–40.

Lin, J.F., Struzhkin, V.V., Mao, H.k., Hemley, R.J., Chow, P., Hu, M.Y., Li, J., 2004b. Magnetic transition in compressed Fe_3C from x-ray emission spectroscopy. Phys. Rev. B 70, 212405.

Lin, J.F., Struzhkin, V.V., Sturhahn, W., Huang, E., Zhao, J., Hu, M.Y., Alp, E.E., Mao, H.k., Boctor, N.Z., Hemley, R.J., 2003b. Sound velocities of iron–nickel and iron–silicon alloys at high pressures. Geophys. Res. Lett. 30, 2122.

Liu, J., Li, J., Ikuta, D., 2016a. Elastic softening in Fe_7C_3 with implications for Earth's deep carbon reservoirs. J. Geophys. Res. 121, 1514–1524.

Liu, J., Lin, J.F., Prakapenka, V.B., Prescher, C., Yoshino, T., 2016b. Phase relations of Fe_3C and Fe_7C_3 up to 185 GPa and 5200 K: implication for the stability of iron carbide in the Earth's core. Geophys. Res. Lett. 43, 12,415–12,422.

Lord, O., Walter, M., Dasgupta, R., Walker, D., Clark, S.M., 2009. Melting in the Fe–C system to 70 GPa. Earth Planet. Sci. Lett. 284, 157–167.

Mao, H., Xu, J., Bell, P.M., 1986. Calibration of the ruby pressure gauge to 800 kbar under quasi-hydrostatic conditions. J. Geophys. Res., Solid Earth 91, 4673–4676.

Mao, H., Xu, J., Struzhkin, V.V., Shu, J., Hemley, R.J., Sturhahn, W., Hu, M.Y., Alp, E.E., Vočadlo, L., Alfé, D., Price, G., Gillan, M.J., Schwoerer-Böhning, M., Hausermann, D., Eng, P., Shen, G., Giefers, H., Lübbers, R., Wortmann, G., 2001. Phonon density of states of iron up to 153 gigapascals. Science 292, 914–916.

Mao, Z., Lin, J.F., Liu, J., Alatas, A., Gao, L., Zhao, J., Mao, H., 2012. Sound velocities of Fe and Fe–Si alloy in the Earth's core. Proc. Natl. Acad. Sci. USA 109, 10239–10244.

Martorell, B., Vočadlo, L., Brodholt, J., Wood, I.G., 2013. Strong premelting effect in the elastic properties of hcp-Fe under inner-core conditions. Science 342, 466–468.

Mookherjee, M., 2011. Elasticity and anisotropy of Fe_3C at high pressures. Am. Mineral. 96, 1530–1536.

Murphy, C.A., Jackson, J.M., Sturhahn, W., 2013. Experimental constraints on the thermodynamics and sound velocities of hcp-Fe to core pressures. J. Geophys. Res. 118, 1999–2016.

Nakajima, Y., Takahashi, E., Suzuki, T., Funakoshi, K.I., 2009. 'Carbon in the core' revisited. Phys. Earth Planet. Inter. 174, 202–211.

Ono, S., Mibe, K., 2010. Magnetic transition of iron carbide at high pressures. Phys. Earth Planet. Inter. 180, 1–6.

Prescher, C., Dubrovinsky, L.S., Bykova, E., Kantor, A., Nakajima, Y., Miyajima, N., Sinmyo, R., Prakapenka, V., Hanfland, M., 2015. High Poisson's ratio of Earth's inner core explained by carbon alloying. Nat. Geosci. 8, 220–223.

Raza, Z., Shulumba, N., Caffrey, N.M., Dubrovinsky, L.S., Abrikosov, I.A., 2015. First-principles calculations of properties of orthorhombic iron carbide Fe_7C_3 at the Earth's core conditions. Phys. Rev. B 91, B04201.

Sata, N., Sata, N., Hirose, K., Hirose, K., Shen, G., Shen, G., Nakajima, Y., Nakajima, Y., Ohishi, Y., Hirao, N., 2010. Compression of FeSi, Fe_3C, $Fe_{0.95}O$, and FeS under the core pressures and implication for light element in the Earth's core. J. Geophys. Res. 115, B09204.

Shahar, A., Schauble, E.A., Caracas, R., Gleason, A.E., Reagan, M.M., Xiao, Y., Shu, J., Mao, W., 2016. Pressure-dependent isotopic composition of iron alloys. Science 352, 580–582.

Shibazaki, Y., Ohtani, E., Fukui, H., Sakai, T., Kamada, S., Ishikawa, D., Tsutsui, S., Baron, A.Q.R., Nishitani, N., Hirao, N., Takemura, K., 2012. Sound velocity measurements in dhcp-FeH up to 70 GPa with inelastic X-ray scattering: implications for the composition of the Earth's core. Earth Planet. Sci. Lett. 313–314, 79–85.

Singh, S.C., Taylor, M.A.J., Montagner, J.P., 2000. On the presence of liquid in Earth's inner core. Science 287, 2471.

Song, X., Helmberger, D.V., 1993. Anisotropy of the Earth's inner core. Geophys. Res. Lett. 20, 2591–2594.

Sturhahn, W., 2000. CONUSS and PHOENIX: evaluation of nuclear resonant scattering data. Hyperfine Interact. 125, 149–172.

Sturhahn, W., Jackson, J.M., 2007. Geophysical applications of nuclear resonant spectroscopy. In: Special Paper 421: Advances in High-Pressure Mineralogy. Geological Society of America, pp. 157–174.

Vanko, G., Neisius, T., Molnár, G., Renz, F., Kárpáti, S., Shukla, A., de Groot, F.M.F., 2006. Probing the 3d spin momentum with X-ray emission spectroscopy: the case of molecular-spin transitions. J. Phys. Chem. B 110, 11647–11653.

Vočadlo, L., 2007. Ab initio calculations of the elasticity of iron and iron alloys at inner core conditions: evidence for a partially molten inner core? Earth Planet. Sci. Lett. 254, 227–232.

Vočadlo, L., Brodholt, J., Dobson, D.P., Knight, K., Marshall, W., Price, G.D., Wood, I.G., 2002. The effect of ferromagnetism on the equation of state of Fe_3C studied by first-principles calculations. Earth Planet. Sci. Lett. 203, 567–575.

Wood, B.J., 1993. Carbon in the core. Earth Planet. Sci. Lett. 117, 593–607.

Wood, B.J., Li, J., Li, J., Shahar, A., Shahar, A., 2013. Carbon in the core: its influence on the properties of core and mantle. Rev. Mineral. Geochem. 75, 231–250.